

S_4 Symmetric Microscopic Model for Iron-Based Superconductors

Jiangping Hu^{1,2} and Ningning Hao^{1,2}

¹*Beijing National Laboratory for Condensed Matter Physics,*

Institute of Physics, Chinese Academy of Sciences, Beijing 100080, China

²*Department of Physics, Purdue University, West Lafayette, Indiana 47907, USA*

Although iron-based superconductors are multi-orbital systems with complicated band structures, we demonstrate that the low energy physics which is responsible for high- T_c superconductivity is essentially governed by an effective two-orbital Hamiltonian near half filling. This underlining electronic structure is protected by the S_4 symmetry. With repulsive or strong next nearest neighbor antiferromagnetic exchange interactions, the model results in a robust A_{1g} s -wave pairing which can be exactly mapped to the d -wave pairing observed in cuprates. The classification of the superconducting(SC) states according to the S_4 symmetry leads to a natural prediction of the existence of two different phases named A and B phases. In the B phase, the superconducting order has an overall sign change along c -axis between the top and bottom As(Se) planes in a single Fe-(As)Se trilayer structure, which is an analogy of the sign change under the 90° degree rotation in the d -wave SC state of cuprates. Our derivation provides a unified understanding of iron-pnictides and iron-chalcogenides, and suggests that cuprates and iron-based superconductors share identical high- T_c superconducting mechanism.

I. INTRODUCTION

Since the discovery of iron-based superconductors[1–4], there has been considerable controversy over the choice of the appropriate microscopic Hamiltonian[5, 6]. The major reason behind such a controversy is the complicated multi d -orbital electronic structure of the materials. Although the electronic structure has been modeled by using different numbers of orbitals, ranging from minimum two orbitals[7], three orbitals[8], to all five d orbitals[9, 10], a general perception has been that any microscopic model composed of less than all five d -orbitals and ten bands is insufficient[6]. Such a perception has blocked the path to understand the superconducting mechanism because of the difficulty in identifying the key physics responsible for high T_c . Realistically, in a model with five orbitals, it is very difficult for any theoretical calculation to make meaningful predictions in a controllable manner.

Iron-based superconductors include two families, iron-pnictides[1–3] and iron-chalcogenides[4]. They share many intriguing common properties. They both have the highest T_c s around 50K[2, 5, 11–13]. The superconducting gaps are close to isotropic around Fermi surfaces[14–19] and the ratio between the gap and T_c , $2\Delta/T_c$, are much larger than the BCS ratio, 3.52, in both families. However, the electronic structures in the two families, in particular, the Fermi surface topologies, are quite different in the materials reaching high T_c . The hole pockets are absent in iron-chalcogenides but present in iron-pnictides[14, 17–19]. The presence of the hole pockets has been a necessity for superconductivity in the majority of studies and models which deeply depend on the properties of Fermi surfaces. Therefore, the absence of the hole pockets in iron-chalcogenides causes a strong debate over whether both families belong to the same category that shares a common superconducting mechanism. Without a clear microscopic picture of the underlining electronic

structure, such a debate can not be settled.

Observed by angle-resolved photoemission microscopy (ARPES), a very intriguing property in the SC states of iron-pnictides is that the SC gaps on different Fermi surfaces are nearly proportional to a simple form factor $\cos k_x \cos k_y$ in reciprocal space. This form factor has been observed in both 122[14, 15, 20, 21] and 111[22, 23] families of iron-pnictides. Just like the d -wave form factor $\cos k_x - \cos k_y$ in cuprates, such a form factor indicates that the pairing between two next nearest neighbour iron sites in real space dominates. In a multi orbital model, many theoretical calculations based on weak coupling approaches have shown that the gap functions are very sensitive to detailed band structures and vary significantly when the doping changes[6, 24–28]. The robustness of the form factor has been argued to favor strong coupling approaches which emphasize electron-electron correlation or the effective next nearest neighbour (NNN) antiferromagnetic (AF) exchange coupling J_2 [29–35] as a primary source of the pairing force. However, realistically, it is very difficult to imagine such a local exchange interaction remains identical between all d -orbital electrons if a multi d -orbital model is considered.

In this paper, we demonstrate that the underlining electronic structure in iron-based superconductors, which is responsible for superconductivity at low energy, is essentially governed by a two orbital model obeying the S_4 symmetry. The two orbital model includes two nearly degenerated single-orbital parts that can be mapped to each other under the S_4 transformation. This electronic structure stems from the fact that the dynamics of d_{xz} and d_{yz} orbitals are divided into two groups that are separately coupled to the top and bottom As(Se) planes in a single Fe-(As)Se trilayer structure. The two groups can thus be treated as a S_4 iso-spin. The dressing of other orbitals in the d_{xz} and d_{yz} orbitals can not alter the symmetry characters.

The underlining electronic structure becomes transpar-

ent after performing a gauge mapping in the five orbital model[10]. The gauge mapping also reveals the equivalence between the A_{1g} s -wave pairing and the d -wave pairing. After the gauge mapping, the band structure for each S_4 iso-spin component is characterized by Fermi surfaces located around the anti d -wave nodal points in Brillouin zone, corresponding to the sublattice periodicity of the bipartite iron square lattice as shown in Fig.1(a). In the presence of an AF exchange coupling J_2 or an effective on-site Hubbard interaction, the d -wave pairing defined in the sublattices can be argued to be favored, just like the case in cuprates. The d -wave pairing symmetry maps reversely to a A_{1g} s -wave pairing in the original gauge setting. These results provide a unified microscopic understanding of iron-pnictides and iron-chalcogenides and explain why an s -wave SC state without the sign change on Fermi surfaces in iron chalcogenides driven by repulsive interaction can be so robust. More intriguingly, since the different gauge settings do not alter any physical measurements, the results suggest that in the A_{1g} s -wave state, for each S_4 iso-spin component, there is a hidden sign change between the top As(Se) and the bottom As(Se) planes along c -axis.

The S_4 symmetry adds a new symmetry classification to the SC states. For example, even in the A_{1g} s -wave pairing state, there are two different phases called A and B phases, with respect to the S_4 symmetry. In the A phase, the relative SC phase between the two S_4 iso-spin components is zero while in the B phase, it is π . Therefore, there is an overall π phase shift between the top As(Se) and the bottom As(Se) planes in the B phase along the c -axis. Such a sign change should be detectable experimentally. This property makes iron-based superconductors useful in many SC device applications. An experimental setup, similar to those for determining the d -wave pairing in cuprates[36–38], is proposed to detect the π phase shift. The detection of the sign change will strongly support that cuprates and iron-based superconductors share identical microscopic superconducting mechanism and will establish that repulsive interactions are responsible for superconductivity.

The paper is organized in the following way. In Section II, we perform a gauge mapping and discuss the emergence of the underlining electronic structure. In Section III, we show that the underlining electronic structure can be constructed by a two orbital model obeying the S_4 symmetry and discuss many general properties in the model. In Section IV, we discuss the classification of the SC states under the S_4 symmetry and propose a measurement to detect the π phase shift along c -axis between the top and bottom As(se) planes. In Section V, we discuss the analogy between iron-based superconductors and cuprates.

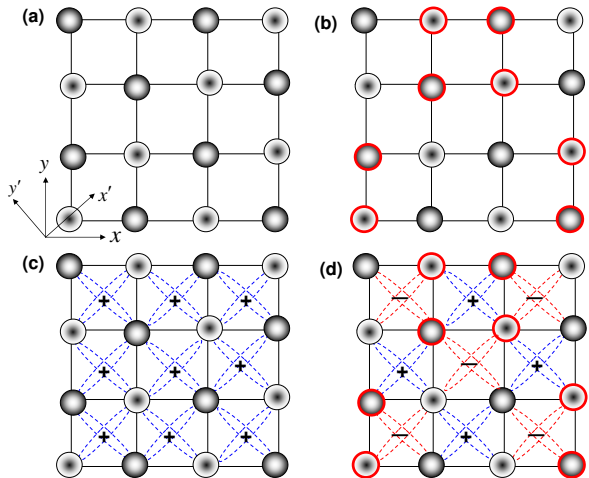


FIG. 1. (a) the square lattice structure of a single iron layer: one cell includes two Fe ions identified with different filled black balls which form two sublattices. We use $x - y$ coordinate to mark the original tetragonal lattices and $x' - y'$ to mark the sublattice direction. (b) the gauge transformation is illustrated. The balls with red circles are affected by the gauge transformation. (c) and (d) the mapping from the s -wave to the d -wave pairing symmetry by the gauge transformation.

II. GAUGE MAPPING AND THE EQUIVALENCE OF s -WAVE AND d -WAVE PAIRING

Gauge Mapping: We start to ask whether there is an unidentified important electronic structure in iron-based superconductors in a different gauge setting. Giving a translational invariant Hamiltonian that describes the electronic band structure of a Fe square lattice,

$$\hat{H}_0 = \sum_{ij, \alpha\beta, \sigma} t_{ij, \alpha\beta} \hat{f}_{i\alpha, \sigma}^+ \hat{f}_{j\beta, \sigma}, \quad (1)$$

where i, j label Fe sites, α, β label orbitals and σ labels spin. We consider the following gauge transformation. As shown in Fig.1(a,b), we group four neighbouring iron sites to form a super site and mark half super sites by red color. The gauge transformation, \hat{U} , adds a minus sign to all Fermionic operators $\hat{f}_{i\alpha, \sigma}$ at every site i marked by red color. After the transformation, the Hamiltonian becomes

$$\hat{H}'_0 = \hat{U}^+ \hat{H}_0 \hat{U}. \quad (2)$$

The gauge mapping operator \hat{U} is a unitary operator so that the eigenvalues of \hat{H}_0 are not changed after the gauge transformation. It is also important to notice that the mapping does not change standard interaction terms, such as conventional electron-electron interactions and spin-spin exchange couplings. Namely, for a general Hamiltonian including interaction terms \hat{H}_I , under the

mapping,

$$\hat{H} = \hat{H}_0 + \hat{H}_I \rightarrow \hat{H}' = \hat{U}^\dagger \hat{H} \hat{U} = \hat{H}'_0 + \hat{H}'_I. \quad (3)$$

It is also easy to see that every unit cell of the lattice in the new gauge setting includes four iron sites. The original translational invariance of a Fe-As(Se) layer has two Fe sites per unit cell. As we will show in the following section, the doubling of the unit cell matches the true hidden unit cell in the electronic structure when the orbital degree of freedom is considered. This is the fundamental reason that the new gauge happens to reveal the underlining electronic structure.

Equivalence of s -wave and d -wave pairing: The gauge mapping has another important property. As shown in Fig.1(c,d), this transformation maps the A_{1g} s -wave $\cos(k_x)\cos(k_y)$ pairing symmetry in the original Fe lattice to a familiar d -wave $\cos k'_x - \cos k'_y$ pairing symmetry defined in the two sublattices, where (k_x, k_y) and (k'_x, k'_y) label momentum in Brillouin zones of the origin lattice and sublattice respectively. A similar mapping has been discussed in the study of a two-orbital iron ladder model[35, 39] to address the equivalence of s -wave and d -wave pairing symmetry in one dimension.

In an earlier paper[32], one of us and his collaborator suggested a phenomenological necessity for achieving high T_c and selecting pairing symmetries: when the pairing is driven by a local AF exchange coupling, the pairing form factor has to match the Fermi surface topology in reciprocal space. If this rule is valid and the iron-based superconductors are in the A_{1g} s -wave state, we expect that the Fermi surfaces after the gauge mapping should be located in the d -wave anti-nodal points in the sublattice Brillouin zone, which is indeed the case as we will show in the following.

Band structures after gauge mapping: There have been various tight binding models to represent the band structure of \hat{H}_0 . In Fig.2, we plot the band structure of \hat{H}_0 and the corresponding \hat{H}'_0 for two different models: a maximum five-orbital model for iron-pnictides[10], and a three-orbital model constructed for electron-overdoped iron-chalcogenides[30].

As shown in Fig.2, although there are subtle differences among the band structures of H'_0 , striking common features are revealed for both models. First, exactly as expected, all Fermi surfaces after the gauge mapping are relocated around X' , the anti-nodal points in a standard d -wave superconducting state in the sublattice Brillouin zone. This is remarkable because a robust d -wave superconducting state can be argued to be favored in such a Fermi surface topology in the presence of repulsive interaction or nearest neighbour (NN) AF coupling in the sublattice[32, 40]. If we reversely map to the original gauge, the original Hamiltonian must have a robust s -wave pairing symmetry. Therefore, an equivalence between the A_{1g} s -wave and the d -wave pairing is clearly established by the gauge mapping.

Second, the bands previously located at the different places on the Fermi surface are magically linked in the

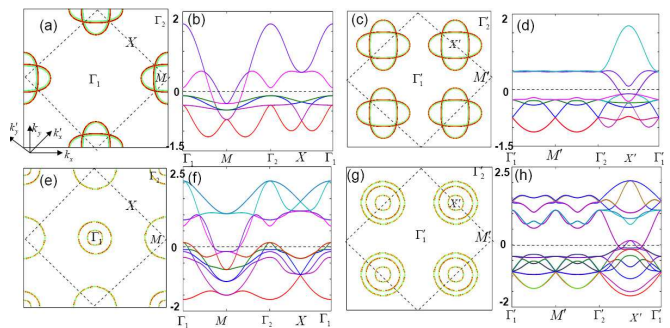


FIG. 2. (Three[30], five[10]) orbital models: (a,e) the Fermi surfaces, (b,f) the band dispersion along the high symmetry lines, (c,g) the Fermi surfaces after the gauge transformation, (d,h) the band dispersions along the high symmetry lines after the gauge transformation. The hopping parameters can be found in the above two references.

new gauge setting. In particular, the two bands that contribute to electron pockets are nearly degenerate and in the five orbital model, the bands that contribute to hole pockets are remarkably connected to them. Considering the fact that the unit cell has four iron sites in the new gauge setting, this unexpected connections lead us to believe that in the original gauge, there should be just two orbitals which form bands that make connections from lower energy bands to higher energy ones and determine Fermi surfaces. Moreover, the two orbitals should form two groups which provide two nearly degenerate band structures. Finally, since the mapping does not change electron density, Fig.2 reveals the doping level in each structure should be close to half filling.

In summary, the gauge mapping reveals that the low energy physics is controlled by a two orbital model that produces two nearly degenerated bands.

III. THE CONSTRUCTION OF A TWO-ORBITAL MODEL WITH THE S_4 SYMMETRY

With above observations, we move to construct an effective two orbital model to capture the underlining electronic structure revealed by the gauge mapping.

Physical picture: Our construction is guided by the following several facts. First, the d -orbitals that form the bands near the Fermi surfaces are strongly hybridized with the p-orbitals of As(Se). Since the $d_{x'z}$ and $d_{y'z}$ have the largest overlap with the $p_{x'}$ and $p_{y'}$ orbitals, it is natural for us to use $d_{x'z}$ and $d_{y'z}$ to construct the model. Second, in the previous construction of a two-orbital model, the C_{4v} symmetry was used[7]. The C_{4v} symmetry is not a correct symmetry if the hopping parameters are generated through the p-orbitals of As(Se). Considering the As(Se) environment, a correct symmetry for the d -orbitals at the iron-sites is the S_4 symmetry group. Third, there are two As(Se) planes which are sep-

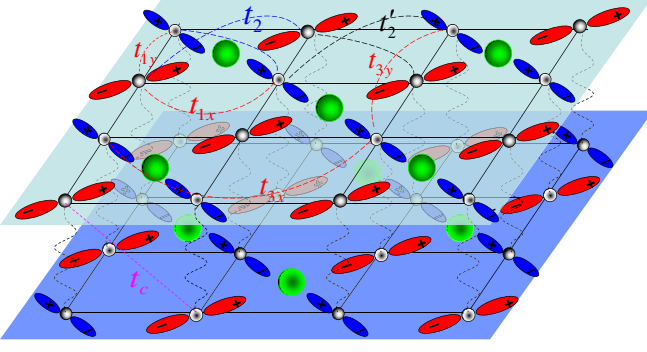


FIG. 3. A sketch of the $d_{x'z}$ and $d_{y'z}$ orbitals, their orientations and their coupling into the two As(Se) layers. The hopping parameters are indicated: the nearest neighbor hopping is marked by $t_{1x,1y}$, the next nearest neighbor hoppings are t_2 and t'_2 due to the broken symmetry along two different diagonal directions, the third NN hopping is marked by $t_{3x,3y}$. The coupling between two layers is marked by the nearest neighbor hopping t_c .

arated in space along c-axis. Since there is little coupling between the p orbitals of the two planes and the hoppings through the p -orbitals are expected to dominate over the direct exchange hoppings between the d -orbitals themselves, the two orbital model essentially could be decoupled into two nearly degenerated one orbital models. Finally, the model should have a translational invariance with respect to the As(Se) plane.

With above guidelines, it is very natural for us to di-

$$\begin{aligned} \hat{H}_{0,one} = & \sum_{k,\sigma} 2[t_{1s}(\cos k_x + \cos k_y) - \frac{\mu}{2} + t_{1d}(\cos k_x - \cos k_y)]\hat{c}_{k\sigma}^+ \hat{c}_{k\sigma} + 4[t_{2s}\cos k_x \cos k_y \hat{c}_{k\sigma}^+ \hat{c}_{k\sigma} + t_{2d}\sin k_x \sin k_y \hat{c}_{k\sigma}^+ \hat{c}_{k+Q\sigma}] \\ & + 2[t_{3s}(\cos 2k_x + \cos 2k_y) + t_{3d}(\cos 2k_x - \cos 2k_y)]\hat{c}_{k\sigma}^+ \hat{c}_{k\sigma} + \dots \end{aligned} \quad (5)$$

We can apply the S_4 transformation on $\hat{H}_{0,one}$ to obtain the tight binding model for the second group. The transformation invariance requires t_{1s}, t_{2d} and t_{3d} to change signs. Therefore, the two-orbital model is described by

$$\begin{aligned} \hat{H}_{0,two} = & \sum_{k\sigma} [4t_{2s}\cos k_x \cos k_y - \mu](\hat{c}_{k\sigma}^+ \hat{c}_{k\sigma} + \hat{d}_{k\sigma}^+ \hat{d}_{k\sigma}) \\ & + 2t_{1s}(\cos k_x + \cos k_y)(\hat{c}_{k\sigma}^+ \hat{c}_{k\sigma} - \hat{d}_{k\sigma}^+ \hat{d}_{k\sigma}) \\ & + 2t_{1d}(\cos k_x - \cos k_y)(\hat{c}_{k\sigma}^+ \hat{c}_{k\sigma} + \hat{d}_{k\sigma}^+ \hat{d}_{k\sigma}) \\ & + 4t_{2d}\sin k_x \sin k_y(\hat{c}_{k\sigma}^+ \hat{c}_{k+Q\sigma} - \hat{d}_{k\sigma}^+ \hat{d}_{k+Q\sigma}) \end{aligned}$$

vide the two d -orbitals into two groups as shown in Fig.3. One group includes the $d_{x'z}$ in the A sublattice and the $d_{y'z}$ in the B sublattice, and the other includes the $d_{x'z}$ in the B sublattice and the $d_{y'z}$ in the A sublattice, where A and B label the two sublattices of the iron square lattice as shown in Fig.1(a). The first group strongly couples to the p -orbitals in the up As(Se) layer and the second group couples to those in the bottom As(Se) layer. We denote $\hat{c}_{i\sigma}$ and $\hat{d}_{i\sigma}$ as Fermionic operators for the two groups respectively at each iron site.

S_4 symmetry and the two-orbital model: Without turning on couplings between the two groups, we seek a general tight binding model to describe the band structure based on the S_4 symmetry. The S_4 transformation maps $\hat{c}_{i\sigma}$ to $\hat{d}_{i\sigma}$. If we define the corresponding operators in momentum space as $\hat{c}_{k\sigma}$ and $\hat{d}_{k\sigma}$, the S_4 transformation takes

$$\begin{pmatrix} \hat{c}_{k\sigma} \\ \hat{d}_{k\sigma} \end{pmatrix} \rightarrow \begin{pmatrix} -\hat{d}_{k'+Q\sigma} \\ \hat{c}_{k'+Q\sigma} \end{pmatrix}, \quad (4)$$

where $k' = (k_y, -k_x)$ and $Q = (\pi, \pi)$ for given $k = (k_x, k_y)$.

Now, we consider a tight binding model for the first group. Here we limit the hopping parameters up to the third NN (TNN). As illustrated in Fig.3, the tight binding model can be approximated by including NN hoppings, t_{1x}, t_{1y} , NNN hoppings, t_2, t'_2 , and TNN hoppings, t_{3x} and t_{3y} . The longer range hoppings can be included if needed. For convenience, we can define $t_{1s} = (t_{1x} + t_{1y})/2$, $t_{1d} = (t_{1x} - t_{1y})/2$, $t_{2s} = (t_2 + t'_2)/2$ and $t_{2d} = (t_2 - t'_2)/2$, $t_{3s} = (t_{3x} + t_{3y})/2$ and $t_{3d} = (t_{3x} - t_{3y})/2$, where the labels, s and d , indicate s -wave (hopping parameter is symmetric under the 90° degree rotation) and d -wave (hopping parameter changes sign under the 90° degree rotation) type hoppings respectively. A general tight binding model can be written as

$$\begin{aligned} & + 2t_{3s}(\cos 2k_x + \cos 2k_y)(\hat{c}_{k\sigma}^+ \hat{c}_{k\sigma} + \hat{d}_{k\sigma}^+ \hat{d}_{k\sigma}) \\ & + 2t_{3d}(\cos 2k_x - \cos 2k_y)(\hat{c}_{k\sigma}^+ \hat{c}_{k\sigma} - \hat{d}_{k\sigma}^+ \hat{d}_{k\sigma}) \\ & + \dots \end{aligned} \quad (6)$$

Now we can turn on the couplings between the two groups. It is straightforward to show that the leading order of the couplings that satisfies the S_4 symmetry is given by

$$\hat{H}_{0,c} = \sum_k 2t_c(\cos k_x + \cos k_y)(\hat{c}_{k\sigma}^+ \hat{d}_{k\sigma} + h.c.). \quad (7)$$

Combining the $\hat{H}_{0,two}$ and $\hat{H}_{0,c}$, we obtain an effective S_4 symmetric two orbital model whose band structure is described by

$$\hat{H}_{0,eff} = \hat{H}_{0,two} + \hat{H}_{0,c}. \quad (8)$$

The \hat{c} and \hat{d} Fermionic operators can be viewed as two

iso-spin components of the S_4 symmetry.

Let's assume t_c to be small and check whether $H_{0,eff}$ can capture the electronic structure at low energy. Ignoring t_c , $H_{0,eff}$ provides the following energy dispersions for the two orbitals,

$$E_{e\pm} = \epsilon_k \pm 2t_{3d}(\cos 2k_x - \cos 2k_y) + 4\sqrt{t_{2d}^2 \sin^2 x \sin^2 y + \left[\frac{t_{1s}(\cos k_x + \cos k_y) \pm t_{1d}(\cos k_x - \cos k_y)}{2}\right]^2}, \quad (9)$$

$$E_{h\pm} = \epsilon_k \pm 2t_{3d}(\cos 2k_x - \cos 2k_y) - 4\sqrt{t_{2d}^2 \sin^2 x \sin^2 y + \left[\frac{t_{1s}(\cos k_x + \cos k_y) \pm t_{1d}(\cos k_x - \cos k_y)}{2}\right]^2}, \quad (10)$$

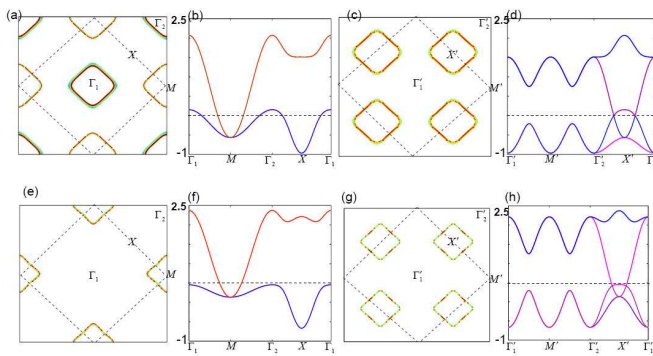


FIG. 4. The Fermi surfaces of each component when only parameters t_{1s} , t_{2d} and t_{2s} are considered. The layout exactly follows Fig.2. The parameters are $t_1 = 0.24$, $t_2 = 0.52$ and $\mu = -0.273$. The only different parameter between (a) and (e) is t'_2 with $t'_2 = -0.1$ in (a) and $t'_2 = -0.2$ in (e).

where $\epsilon_k = 4t_{2s}\cos k_x \cos k_y + 2t_{3s}(\cos 2k_x + \cos 2k_y) - \mu$.

We find that $E_{e\pm}$ can capture the electron pockets at M points and $E_{h\pm}$ can capture the hole pockets at Γ points. Based on the previous physical picture, t_{1s} , t_{2s} and t_{2d} should be the largest parameters because they are generated through the p-orbitals. In Fig.4, we show that by just keeping these three parameters, the model is already good enough to capture the main characters of the bands contributing to Fermi surfaces in the five-orbital model. After performing the same gauge mapping, this Hamiltonian, as expected, provides pockets located at X' as shown in Fig.4.

General properties of the model: The above model is good enough to quantitatively describe the experimental results measured by ARPES[14, 20, 41–44]. Although the hopping parameters are dominated by t_{1s} , t_{2d} and t_{2s} , other parameters can not be ignored. For example, at the same M points, there is energy splitting between two components, which indicates the existence of a sizable t_{1d} . To match the detailed dispersion of the bands, the TNN hoppings have to be included. The existence of the TNN hoppings may also provide a microscopic jus-

tification for the presence of the significant TNN AFM exchange coupling J_3 measured by neutron scattering in iron-chalcogenides[32, 45, 46].

While the detailed quantitative results for different families of iron-based superconductors will be present elsewhere[41], we plot a typical case for iron-pnictides with parameters $t_{1s} = 0.4$, $t_{1d} = -0.03$, $t_{2s} = 0.3$, $t_{2d} = 0.6$, $t_{3s} = 0.05$, $t_{3d} = -0.05$ and $\mu = -0.3$ in fig.5(a-d). In Fig.5(a,b), the coupling $t_c = 0$. In Fig.5(c,d), $t_c = 0.02$. It is clear that the degeneracy at the hole pockets along $\Gamma - X$ direction is lifted by t_c . The Fermi surfaces in Fig.5 are very close to those in the five orbital model[10]. This result is consistent with our assumption that t_c effectively is small.

There are several interesting properties in the model. First, the model unifies the iron-pnictides and iron-chalcogenides. When other parameters are fixed, reducing t_{2s} or increasing t_{1s} can flatten the dispersion along $\Gamma - M$ direction of $E_{h\pm}$ and cause the hole pocket completely vanishes. Therefore, the model can describe both iron-pnictides and electron-overdoped iron-chalcogenides by varying t_{2s} or t_{1s} .

Second, carefully examining the hopping parameters, we also find that the NNN hopping for each S_4 iso-spin essentially has a d -wave symmetry, namely $|t_{2d}| > t_{2s}$. Since the hole pockets can be suppressed by reducing t_{2s} value, this d -wave hopping symmetry is expected to be stronger in iron chalcogenides than in iron-pnictides.

Third, it is interesting to point out that we can make an exact analogy between the S_4 transformation on its two iso-spin components and the time reversal symmetry transformation on a real 1/2-spin because $S_4^2 = -1$. This analogy suggests in this S_4 symmetric model, the degeneracy at high symmetric points in Brillouin zone is the type of the Kramers degeneracy.

Finally, in this model, if the orbital degree of freedom is included, the true unit cell for each iso-spin component includes four irons. The gauge mapping in the previous section exactly takes a unit cell with four iron sites. Such a match is the essential reason why the low energy physics becomes transparent after the gauge mapping.

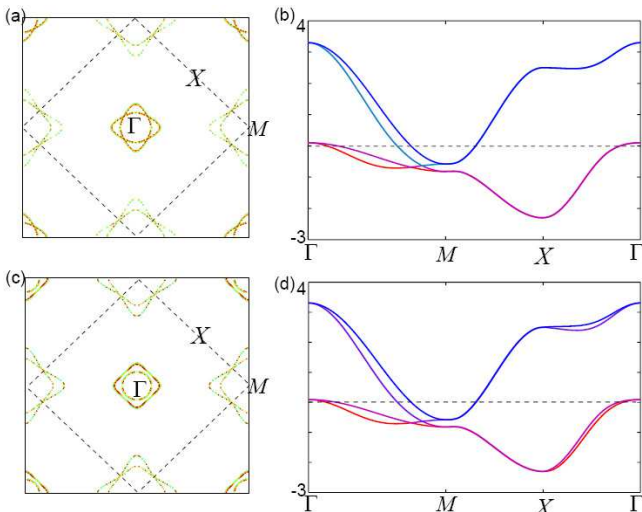


FIG. 5. A typical Fermi surfaces (a), band dispersions (b) resulted from Eq.10 with parameters $t_{1s} = 0.4, t_{1d} = -0.03, t_{2s} = 0.3, t_{2d} = 0.6, t_{3s} = 0.05, t_{3d} = -0.05$ and $\mu = -0.3$. (c) and (d) are corresponding results by adding $t_c = 0.02$ in Eq.7 with the same parameter setting.

The two-orbital model with interactions: By projecting all interactions into these two effective orbital model, a general effective model that describes iron-based superconductors obeying the S_4 symmetry can be written as

$$H_{eff} = H_{0,eff} + U \sum_{i,\alpha=1,2} \hat{n}_{i,\alpha\uparrow} \hat{n}_{i,\alpha\downarrow} + U' \sum_i \hat{n}_{i,1} \hat{n}_{i,2} + J'_H \sum_i \hat{S}_{i,1} \cdot \hat{S}_{i,2} \quad (11)$$

where $\alpha = 1, 2$ labels the S_4 iso-spin, U describes the effective Hubbard repulsion interaction within each component, U' describes the one between them and J'_H describes the effective Hunds coupling. Since the two components couple weakly, we may expect U dominates over U' and J'_H . Then, in the first order approximation, the model could become a single band-Hubbard model near half filling. A similar t-J model can also be discussed within the same context as cuprates[47, 48]. It is clear that the model naturally provides an explanation for the stable NNN AF exchange couplings J_2 observed by neutron scattering[45, 46, 49] and its dominating role in both magnetism and superconductivity[32].

Reduction of the symmetry from D_{2d} to S_4 The true lattice symmetry in a $Fe - As(Se)$ trilayer is the D_{2d} point group, where S_4 is a subgroup of the D_{2d} . In the D_{2d} group, besides the S_4 invariance, the reflection operator σ_v with respect to the $x' - z$ plane is also invariant. The reflection imposes an additional requirement

$$\begin{pmatrix} \hat{c}_{k\sigma} \\ \hat{d}_{k\sigma} \end{pmatrix} \rightarrow \begin{pmatrix} \hat{c}_{k''+Q\sigma} \\ -\hat{d}_{k''+Q\sigma} \end{pmatrix}, \quad (12)$$

where $k'' = (k_y, k_x)$. It is easy to see that if we force the D_{2d} symmetry, the reflection σ_v invariance requires

$t_{1s} = 0$. However, without such a reflection invariance, this term is allowed, which is the case when only the S_4 symmetry remains.

The existence of t_{1s} suggests that σ_v symmetry must be broken in an effective model. However, since σ_v symmetry appears to be present, it is natural to ask what mechanism can break σ_v . While a detailed study of this symmetry breaking is in preparation[50], we give a brief analysis. Among the five d-orbitals, $d_{xy}, d_{x^2-y^2}$ and d_{z^2} belong to one dimensional representations of the D_{2d} group. In fact, for these three orbitals, the D_{2d} group is equivalent to C_{4v} group. In other words, the As(Se) separation along c-axis has no effect on the symmetry of the kinematics of the three orbitals if the couplings to the other two orbitals, d_{xz} and d_{yz} , are not included. Therefore, for these three orbitals, the unit cell is not doubled by As(Se) atoms and the band structure is intrinsically one iron per unit cell even if the hoppings generated through p-orbitals of As(Se) are important. However, for d_{xz} and d_{yz} orbitals, if the hoppings through p-orbitals of As(Se) are dominant, the unit cell is doubled by As(Se) atoms and the band structure is intrinsically folded. From Eq.12, after the S_4 symmetry is maintained, the σ_v symmetry operations simply map the reduced Brillouin zone to the folded part. If the couplings between the above two groups of orbitals are turned on, the effective two orbitals that describe the low energy physics near Fermi surfaces are not pure d_{xz}, d_{yz} orbitals any more. In particular, they are heavily dressed by d_{xy} orbitals as shown in ARPES[51–54]. Therefore, the effective two orbitals can only keep the S_4 symmetry and the σ_v symmetry has to be broken.

Another possibility of the generation of the t_{1s} hopping may stem from the following virtual hopping processes: one electron first hops from the p_x to the d_{xz} , then, an electron in the p_y at the same As(Se) site can hop to the p_x , finally, an electron in the d_{yz} orbital hops to the p_y . In such a process, the reflection symmetry is broken due to the existence of the hopping between the p_x and p_y orbitals at the same As(Se) site when the two orbitals host total 3 electrons, which is possible if onsite Hubbard interaction U in p orbitals is large so that the degeneracy of p_x and p_y is broken, a result of the standard Jahn-Teller effect.

The coupling between two S_4 iso-spins and S_4 symmetry breaking: The couplings between the two iso-spins can either keep the S_4 symmetry or break it. Without breaking the translational symmetry, the coupling between two orbitals can be written as

$$\hat{H}_c = \sum_{k,\alpha} f_\alpha(k) \hat{G}_\alpha(k) + \sum_{k,\bar{\alpha}} f_{\bar{\alpha}}(k) \hat{G}_{\bar{\alpha}}(k) \quad (13)$$

where $G_\alpha(k)$ and $G_{\bar{\alpha}}(k)$ are operators constructed according to the S_4 one dimensional representations as follows,

$$G_1(k) = \sum_{\sigma} c_{k\sigma}^+ \hat{d}_{k\sigma} + c_{k+Q\sigma}^+ \hat{d}_{k+Q\sigma} + h.c. \quad (14)$$

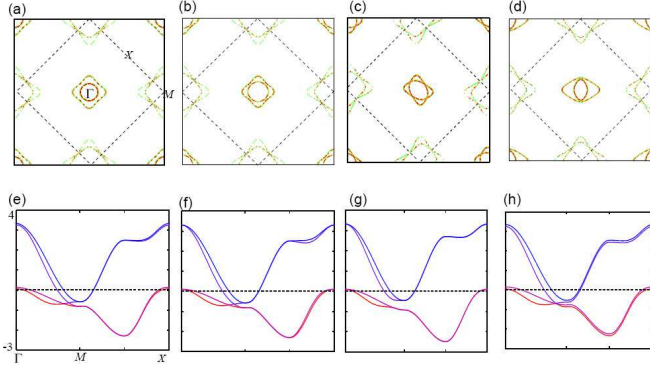


FIG. 6. Fermi surfaces and band dispersions in the presence of the S_4 symmetry breaking: (a, e) $t_{b1} = 0.005$ in Eq. 22; (b, f) $t_{bt} = 0.05$ in Eq. 23; (c, g) $t_{bo} = 0.05$ in Eq. 24; (d, h) $t_{bso} = 0.05$ in Eq. 25. Other parameters are the same as in Fig.5.

$$G_2(k) = \sum_{\sigma} c_{k\sigma}^+ \hat{d}_{k\sigma} - c_{k+Q\sigma}^+ \hat{d}_{k+Q\sigma} + h.c. \quad (15)$$

$$G_3(k) = \sum_{\sigma} c_{k\sigma}^+ \hat{d}_{k+Q\sigma} + c_{k+Q\sigma}^+ \hat{d}_{k\sigma} + h.c. \quad (16)$$

$$G_4(k) = \sum_{\sigma} c_{k\sigma}^+ \hat{d}_{k+Q\sigma} - c_{k+Q\sigma}^+ \hat{d}_{k\sigma} + h.c. \quad (17)$$

$$G_{\bar{1}}(k) = \sum_{\sigma} i(c_{k\sigma}^+ \hat{d}_{k\sigma} + c_{k+Q\sigma}^+ \hat{d}_{k+Q\sigma} - h.c.) \quad (18)$$

$$G_{\bar{2}}(k) = \sum_{\sigma} i(c_{k\sigma}^+ \hat{d}_{k\sigma} - c_{k+Q\sigma}^+ \hat{d}_{k+Q\sigma} - h.c.) \quad (19)$$

$$G_{\bar{3}}(k) = \sum_{\sigma} i(c_{k\sigma}^+ \hat{d}_{k+Q\sigma} + c_{k+Q\sigma}^+ \hat{d}_{k\sigma} - h.c.) \quad (20)$$

$$G_{\bar{4}}(k) = \sum_{\sigma} i(c_{k\sigma}^+ \hat{d}_{k+Q\sigma} - c_{k+Q\sigma}^+ \hat{d}_{k\sigma} - h.c.) \quad (21)$$

We discuss a few examples that can cause the S_4 symmetry breaking,

$$H_{b1} = \sum_k 2t_{b1}(\cos k_x + \cos k_y)(\hat{c}_{k\sigma}^+ \hat{d}_{k+Q\sigma} + h.c.) \quad (22)$$

$$H_{bt} = \sum_k 4it_{bt} \sin k_x \sin k_y (\hat{c}_{k\sigma}^+ \hat{d}_{k+Q\sigma} - h.c.) \quad (23)$$

$$H_{bo} = \sum_k t_{bo}(\hat{c}_{k\sigma}^+ \hat{c}_{k+Q\sigma} - d_{k\sigma}^+ \hat{d}_{k+Q\sigma}) \quad (24)$$

$$H_{bso} = \sum_k t_{bso}(\hat{c}_{k\sigma}^+ \hat{c}_{k\sigma} - d_{k\sigma}^+ \hat{d}_{k\sigma}). \quad (25)$$

t_{b1} term breaks the S_4 symmetry to lift the degeneracy at Γ point, t_{bt} breaks the time reversal symmetry, t_{bo} indicates a ferro-orbital ordering and t_{bso} indicates a staggered orbital ordering. These terms can be generated either spontaneously or externally and their effects can be explicitly observed in the change of the band structure and degeneracy lifting as shown in Fig.6, where the changes of band structures and Fermi surfaces due to the symmetry breaking terms are plotted. It is fascinating to

study how the interplay between the S_4 symmetry and other broken symmetries in this system in future.

IV. THE CLASSIFICATION OF THE SUPERCONDUCTING ORDERS ACCORDING TO THE S_4 SYMMETRY

The presence of the S_4 symmetry brings a new symmetry classification of the superconducting phases. The S_4 point group has four one-dimensional representations, including A , B and $2E$. In the A state, the S_4 symmetry is maintained. In the B state, the state changes sign under the S_4 transformation. In the $2E$ state, the state obtains a $\pm\pi/2$ phase under the S_4 transformation. Therefore, the $2E$ state breaks the C_2 rotational symmetry as well as the time reversal symmetry.

Since the S_4 transformation includes two parts, a 90° degree rotation and a reflection along c-axis, the S_4 symmetry classification leads to a natural correlation between the rotation in a-b plane and c-axis reflection symmetries in a SC state. In the A-phase, rotation and c-axis reflection can be both broken, while in the B-phase, one and only one of them can be broken. This correlation, in principle, may be observed by applying external symmetry breaking. For example, even in the A-phase and the rotation symmetry is not broken, we may force the c-axis phase-flip to obtain the phase change in the a-b plane.

As shown in this paper, the iron-based superconductors are rather unique with respect to the S_4 symmetry. It has two iso-spin components governed by the symmetry. This iso-spin degree of freedom and the interaction between them could lead to many novel phases. The future study can explore these possibilities.

Here we specifically discuss the S_4 symmetry aspects in the proposed A_{1g} s-wave state, a most-likely phase if it is driven by the repulsive interaction or strong AF in iron-based superconductors[29] as we have shown earlier. First, let's clarify the terminology issues. The A_{1g} s-wave pairing symmetry is classified according to D_{4h} point group. This classification is not right in the view of the true lattice symmetry. However, for each iso-spin components, we can still use it. Here we treat it as a state that the superconducting order $\Delta \propto \cos k_x \cos k_y$ [29]. Since the A_{1g} phase is equivalent to the d-wave in cuprates in a different gauge setting, the d-wave picture is more transparent regarding the sign change of the superconducting phase in the real space. As shown in Fig.1, the sign of the SC order alternates between neighboring squares in the iron lattice.

Based on the underlining electronic structure revealed here, with respect to the S_4 symmetry, the A_{1g} state can have two different phases, A phase and B phase. In the A phase,

$$\langle \hat{c}_{k\uparrow} \hat{c}_{-k\downarrow} \rangle = \langle \hat{d}_{k\uparrow} \hat{d}_{-k\downarrow} \rangle = \Delta_0 \cos k_x \cos k_y \quad (26)$$

and in the B phase,

$$\langle \hat{c}_{k\uparrow} \hat{c}_{-k\downarrow} \rangle = - \langle \hat{d}_{k\uparrow} \hat{d}_{-k\downarrow} \rangle = \Delta_0 \cos k_x \cos k_y. \quad (27)$$

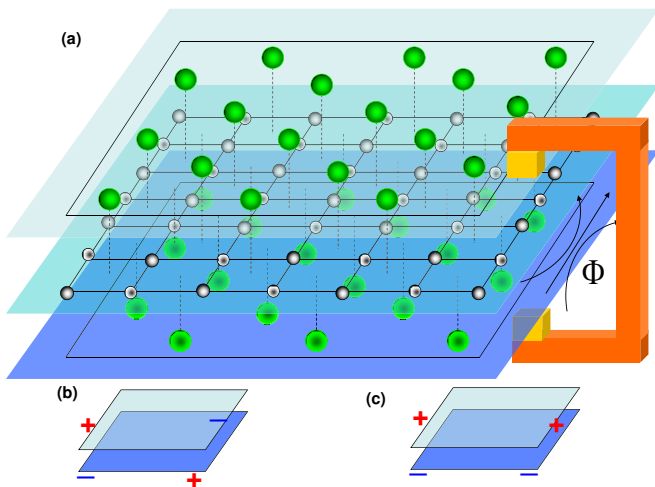


FIG. 7. (a) An illustration of a single Fe-As(Se) layer and the setup for a dc SQUIDS measurement to measure the sign change of the SC phase between top and down As(Se) layers; (b) The phase distribution in the A phase of the A_{1g} s -wave state in the view of a d -wave picture (red for one iso-spin component and blue for the other); (c) The phase distribution in the B phase of the A_{1g} s -wave state.

Therefore, in the view of the d -wave picture, in both A and B phases, the superconducting phase for each component alternates between neighboring squares, which is corresponding to the sign change between the top and bottom planes in the view of the S_4 symmetry. However, in the A phase, since the S_4 symmetry is not violated, the relative phase between the two components are equal to π in space, while in the B phase, the relative phase is zero. A picture of the phase distribution of the two iso-spin components in the A and B phases are illustrated in Fig.7(b,c).

The sign change of the order parameter or the phase shift of π between the top and bottom planes along c -axis can be detected by standard magnetic flux modulation of dc SQUIDS measurements[36]. If we consider a single Fe-As(Se) trilayer structure, which has been successfully grown by MBE recently[11, 12], we can design a standard dc SQUIDS as shown in Fig.7(a) following the similar experimental setup to determine the d -wave pairing in cuprates[36]. For the B phase, there is no question that the design can repeat the previous results in cuprates. However, if the tunneling matrix elements to two components are not symmetric, even in the A phase, this design can obtain the signal of the π phase shift since the two components are weakly coupled and each of them has a π phase shift. For the B phase, the phase shift may be preserved even in bulk materials[55]. However, for the A phase, it will be difficult to detect the phase shift in bulk materials. A cleverer design is needed. Measuring the phase shift between the upper and lower As(Se) planes will be a smoking-gun experiment to verify the model and determine iron-based superconductors and cuprates

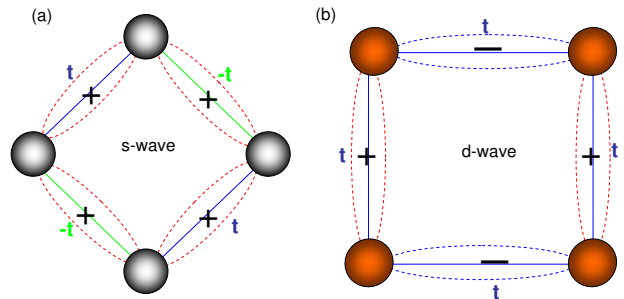


FIG. 8. A sketch of the correlation between the hopping and pairing symmetries for both iron-based superconductors and cuprates.

sharing identical superconducting mechanism.

V. DISCUSSION AND SUMMARY

We have shown that the A_{1g} s -wave pairing in iron-based superconductors is a d -wave pairing in a view of a different gauge setting. This equivalence answers an essential question why a A_{1g} s -wave pairing can be robust regardless of the presence or absence of the hole pockets. With repulsive interactions, a sign changed order parameter in a superconducting state is usually inevitable. This statement, however, is only true when the hopping parameters follow the same lattice symmetry. Gauge transformation can exchange the phases between superconducting order parameters and hopping parameters. In the case of cuprates, the d -wave order parameter can be transformed to a s -wave form by changing hopping parameters to obey d -wave symmetry. As we pointed out earlier, the NNN hopping in our model is close to a d -wave symmetry, rather than a s -wave symmetry. This is the essential reason why the superconducting order can have a s -wave form and be stable in iron-based superconductors. A simple picture of this discussion is illustrated in Fig.8. The vanishing of the hole pockets in electron-overdoped iron-chalcogenides indicates the hopping is even more d -wave like in these materials, a case supporting stronger s -wave pairing, which was indeed observed recently[12, 13]. The presence of the dominant form $\cos k_x \cos k_y$ is also straightly linked to the d -wave pairing form $\cos k'_x - \cos k'_y$ because of the stable AF J_2 coupling, similar to cupates[56]. Moreover, since the different gauge setting does not alter physical measurements, a phase sensitive measurement should reveal a π phase shift in the real space along c -axis for each components in the A_{1g} s -wave state, just like the phase shift along a and b direction in the d -wave pairing state of cuprates.

After obtaining the underlining electronic structure, we can ask how the physics in the cuprates and iron-based superconductors are related to each other. In Table.I, we

| properties | Iron SCs | cuprates |
|---------------------------------|---------------------|-----------------------|
| pairing symmetry | <i>s</i> -wave | <i>d</i> -wave |
| underlining hopping symmetry | <i>d</i> -wave | <i>s</i> -wave |
| dominant pairing form | $\cos k_x \cos k_y$ | $\cos k_x - \cos k_y$ |
| pairing classification symmetry | S_4 | C_4 |
| AF coupling | NNN J_2 | NN J_1 |
| sign change in real space | c-axis | a-b plane |
| filling density | half-filling | half-filling |

TABLE I. A list of the close connections between iron-based superconductors (iron SCs) and cuprates.

list the close relations between two high T_c superconductors. From the table, it is clear that by determining these physical properties of iron-based superconductors listed in the table can help to determine the high T_c superconducting mechanism.

The model completely changes the view of the origin of the generation of sign-changed s^\pm pairing symmetry in iron-pnictides, which were argued in many theories that the origin is the scattering between electron pockets at M and hole pockets at Γ due to repulsive interactions[6, 9]. With the new underlining electronic structure revealed, the analysis of the sign-change should be examined after taking the gauge transformation so that the underlining hopping parameters become symmetric. In this case, the sign change is driven by scatterings between all pockets, including both hole and electron pockets, located at two *d*-wave anti-nodal X' points. Therefore, the scattering between electron and electron pockets is also important.

While the model appears to be rotational invariant due to the S_4 symmetry, the dynamics of each iso-spin component is intrinsically nematic. A small S_4 symmetry breaking can easily lead to an overall electronic nematic state. The electronic nematic state has been observed by many experimental techniques[57] and studied by dif-

ferent theoretical models[58–65]. The underlining electronic structure in the model can provide a straightforward microscopic understanding between the interplay of all different degree of freedoms based on the S_4 symmetry breaking.

It is worth to pointing out that in our model, if t_{1s} is generated by the mixture of different orbital characters, t_{1s} is generally not limited to the NN hopping. It can be a function of k which satisfies $t_{1s}(k) = -t_{1s}(k + Q)$ so that it breaks σ_v symmetry. The value of t_c may be not small. However, both t_{1s} and t_c have very limited effects on the electron pockets. While we may use a different set of t_{1s} and t_c to fit the electronic structure, the key physics in the paper remains the same because the essential physics stems from the NNN hoppings,

In summary, we have shown the underlining electronic structure, which is responsible for superconductivity at low energy in iron-based superconductors, is essentially two nearly degenerated electronic structures governed by the S_4 symmetry. We demonstrate the *s*-wave pairing in iron-based superconductors is equivalent to the *d*-wave in cuprates. A similar conclusion has also been reached in the study of 2-layer Hubbard model[66]. The S_4 symmetry reveals possible new superconducting states and suggests the phase shift in the SC state in real space is along c-axis. These results strongly support the microscopic superconducting mechanism for cuprates and iron-based superconductors are identical, including both iron-pnictides and iron-chalcogenides. Our model establishes a new foundation for understanding and exploring properties of iron based superconductors, a unique, elegant and beautiful class of superconductors.

Acknowledgement: JP thanks H. Ding, D.L. Feng, S. A. Kivelson, P. Coleman, X Dai, Y.P. Wang, EA Kim and F. Wang for useful discussion. JP specially thanks H.Ding, F. Wang, M. Fischer and W. Li for the discussion of the symmetry properties of the model. The work is supported by the Ministry of Science and Technology of China 973 program(2012CB821400) and NSFC-1190024.

-
- [1] Y. Kamihara, T. Watanabe, M. Hirano, and H. Hosono, “Iron-based layered superconductor $LaO_{1-x}F_xFeAs(x = 0.05 - 0.12)$ with $t_c=26$ k,” J. Am. Chem. Soc., **130**, 3296 (2008).
- [2] X. H. Chen, T. Wu, G. Wu, R. H. Liu, H. Chen, and D. F. Fang, “Superconductivity at 43 k in $smFeAs(1-x)f(x)$,” Nature, **453**, 761 (2008).
- [3] G. F. Chen, Z. Li, D. Wu, G. Li, W. Z. Hu, J. Dong, P. Zheng, J. L. Luo, and N. L. Wang, “Superconductivity at 41 k and its competition with spin-density-wave instability in layered $ceO(1-x)f(x)FeAs$,” Phys. Rev. Lett., **100** (2008).
- [4] Jiangang Guo, Shifeng Jin, Gang Wang, Shunchong Wang, Kaixing Zhu, Tingting Zhou, Meng He, and Xiaolong Chen, “Superconductivity in the iron selenide $KxFe_2Se_2$,” Phys. Rev. B, **82**, 180520 (2010).
- [5] P. J. Hirschfeld, M. M. Korshunov, and I. I. Mazin, “Gap symmetry and structure of Fe-based superconductors,” arXiv:1106.3702 (2011).
- [6] David Johnston, “The puzzle of high temperature superconductivity in layered iron pnictides and chalcogenides,” Advances in Physics, **59**, 803–1061 (2010).
- [7] S. Raghu, Xiao-Liang Qi, Chao-Xing Liu, D. J. Scalapino, and Shou-Cheng Zhang, “Minimal two-band model of the superconducting iron oxypnictides,” Phys. Rev. B, **77**, 220503 (2008).
- [8] Patrick A. Lee and Xiao-Gang Wen, “Spin-triplet p-wave pairing in a three-orbital model for iron pnictide superconductors,” Phys. Rev. B., **78**, 144517 (2008).
- [9] I. I. Mazin, D. J. Singh, M. D. Johannes, and M. H. Du, “Unconventional superconductivity with a sign reversal in the order parameter of $LaFeAsO_{1-x}F_x$,” Phys. Rev. Lett.,

- 101**, 57003 (2008).
- [10] Kazuhiko Kuroki, Seiichiro Onari, Ryotaro Arita, Hidetomo Usui, Yukio Tanaka, Hiroshi Kontani, and Hideo Aoki, “Unconventional pairing originating from the disconnected fermi surfaces of superconducting $LaFeAsO_{1-x}F_x$,” *Phys. Rev. Lett.*, **101**, 087004 (2008).
- [11] Defa Liu and et al., “Electronic origin of high temperature superconductivity in single-layer fese superconductor,” *Arxiv:1202.5849* (2012).
- [12] Qing-Yan Wang and et al., “Interface induced high temperature superconductivity in single unit-cell fese films on $srTiO_3$,” *Arxiv:1201.5694* (2012).
- [13] Liling Sun and et al., “Re-emerging superconductivity at 48kelvin in iron chalcogenides,” *Nature*, **10.1038/nature10813** (2012).
- [14] H. Ding and et al., “Observation of fermi-surfacedependent nodeless superconducting gaps in $ba_0.6k_0.4fe_2as_2$,” *Europhysics Lett.*, **83**, 47001 (2008).
- [15] Lin Zhao and et al., “Unusual superconducting gap in $(ba,k)fe_2as_2$ superconductor,” *Chin. Phys. Lett*, **25**, 4402 (2008).
- [16] Y. Zhang, L. X. Yang, F. Chen, B. Zhou, X. F. Wang, X. H. Chen, M. Arita, K. Shimada, H. Namatame, M. Taniguchi, J. P. Hu, B. P. Xie, and D. L. Feng, “Out-of-plane momentum and symmetry dependent superconducting gap in $ba_0.6k_0.4fe_2as_2$,” *Phys. Rev. Lett.*, **105**, 1117003 (2010).
- [17] X.-P. Wang, T. Qian, P. Richard, P. Zhang, J. Dong, H.-D. Wang, C.-H. Dong, M.-H. Fang, and H. Ding, “Strong nodeless pairing on separate electron fermi surface sheets in $(tl, k)fe_1.78se_2$ probed by arpes,” *Europhysics Letters*, **93**, 57001 (2011).
- [18] Y. Zhang, L. X. Yang, M. Xu, Z. R. Ye, F. Chen, C. He, H. C. Xu, J. Jiang, B. P. Xie, J. J. Ying, X. F. Wang, X. H. Chen, J. P. Hu, M. Matsunami, S. Kimura, and D. L. Feng, “Nodeless superconducting gap in $axfe_2se_2$ ($a=k,cs$) revealed by angle-resolved photoemission spectroscopy,” *Nature Materials*, **10**, 273–277 (2011).
- [19] Daixiang Mou, Shanyu Liu, Xiaowen Jia, Junfeng He, Yingying Peng, Lin Zhao, Li Yu, Guodong Liu, Shaolong He, Xiaoli Dong, Jun Zhang, Hangdong Wang, Chiheng Dong, Minghu Fang, Xiaoyang Wang, Qinjun Peng, Zhimin Wang, Shenjin Zhang, Feng Yang, Zuyan Xu, Chuangtian Chen, and X. J. Zhou, “Distinct fermi surface topology and nodeless superconducting gap in a $(tl_0.58rb_0.42)fe_1.72se_2$ superconductor,” *Phys. Rev. Lett.*, **106**, 107001 (2011).
- [20] K. Nakayama T. Takahashi P. Richard, T. Sato and H. Ding, “Fe-based superconductors: an angle-resolved photoemission spectroscopy perspective,” *Reports on Progress in Physics*, **74**, 124512 (2011).
- [21] K. Nakayama, T. Sato, P. Richard, Y.-M. Xu, Y. Sekiba, S. Souma, G. F. Chen, J. L. Luo, N. L. Wang, H. Ding, and T. Takahashi, “Superconducting gap symmetry of $ba_0.6k_0.4fe_2as_2$ studied by angle-resolved photoemission spectroscopy,” *Europhysics Letters*, **85**, 67002 (2009).
- [22] K. Umezawa, Y. Li, H. Miao, K. Nakayama, Z. H. Liu, P. Richard, T. Sato, J. B. He, D. M. Wang, G. F. Chen, H. Ding, T. Takahashi, and S. C. Wang, “Unconventional anisotropic s-wave superconducting gaps of the lifeas iron-pnictide superconductor,” *Phys. Rev. Lett.*, **108** (2012).
- [23] Z. H. Liu, P. Richard, K. Nakayama, G. F. Chen, S. Dong, J. B. He, D. M. Wang, T. L. Xia, K. Umezawa, T. Kawahara, S. Souma, T. Sato, T. Takahashi, T. Qian, Y. B. Huang, N. Xu, Y. B. Shi, H. Ding, and S. C. Wang, “Unconventional superconducting gap in $naf_0(0.95)co(0.05)as$ observed by angle-resolved photoemission spectroscopy,” *Phys. Rev. B.*, **84** (2011).
- [24] Fa Wang, Hui Zhai, Ying Ran, Ashvin Vishwanath, and Dung-Hai Lee, “Functional renormalization-group study of the pairing symmetry and pairing mechanism of the feas-based high-temperature superconductor,” *Phys. Rev. Lett.*, **102**, 47005 (2009).
- [25] R. Thomale, C. Platt, J. P. Hu, C. Honerkamp, and B. A. Bernevig, “Functional renormalization-group study of the doping dependence of pairing symmetry in the iron pnictide superconductors,” *Phys. Rev. B.*, **80**, 180505 (2009).
- [26] Ronny Thomale, Christian Platt, Werner Hanke, Jiangping Hu, and B. Andrei Bernevig, “Exotic d-wave superconductivity in strongly hole doped $k(x)ba(1-x)fe_2as_2$,” *Phys. Rev. Lett.*, **107**, 117001 (2011).
- [27] A. V. Chubukov, D. V. Efremov, and I. Eremin, “Magnetism, superconductivity, and pairing symmetry in iron-based superconductors,” *Phys. Rev. B*, **78**, 134512 (2008).
- [28] Vladimir Cvetkovic and Zlatko Tesanovic, “Valley density-wave and multiband superconductivity in iron-based pnictide superconductors,” *Phys. Rev. B.*, **80**, 24512 (2009).
- [29] K. J. Seo, B. A. Bernevig, and J. P. Hu, “Pairing symmetry in a two-orbital exchange coupling model of oxypnictides,” *Phys. Rev. Lett.*, **101**, 206404 (2008).
- [30] Chen Fang, Yang-Le Wu, Ronny Thomale, B. Andrei Bernevig, and Jiangping Hu, “Robustness of s-wave pairing in electron-overdoped $A_{1-y}Fe_{2-x}Se_2$,” *Phys. Rev X*, **1**, 011009 (2011).
- [31] Qimiao Si and Elihu Abrahams, “Strong correlations and magnetic frustration in the high t_c iron pnictides,” *Phys. Rev. Lett.*, **101**, 76401 (2008).
- [32] Jiangping Hu and Hong Ding, “Local antiferromagnetic exchange and collaborative fermi surface as key ingredients of high temperature superconductors,” *Scientific Reports* (2012).
- [33] Jiangping Hu, Bao Xu, Wuming Liu, Ningning Hao, and Yupeng Wang, “An unified minimum effective model of magnetism in iron-based superconductors,” *Phys. Rev. B*, **85**, 144403 (2012).
- [34] Xiaoli Lu, Chen Fang, Wei-Feng Tsai, Yongjin Jiang, and Jiangping Hu, “S-wave superconductivity with orbital dependent sign change in the checkerboard models of iron-based superconductors,” *Phys. Rev B*, **85**, 054505 (2012).
- [35] E. Berg, S. A. Kivelson, and D. J. Scalapino, “Properties of a diagonal two-orbital ladder model of the iron pnictide superconductors,” *Phys. Rev. B.*, **81**, 172504 (2010).
- [36] D. A. Wollman, D. J. Vanharlingen, W. C. Lee, D. M. Ginsberg, and A. J. Leggett, “Experimental-determination of the superconducting pairing state in $ybco$ from the phase coherence of $ybco-pb$ dc squids,” *Phys. Rev. Lett.*, **71**, 2134 (1993).
- [37] D. J. Van Harlingen, “Phase-sensitive tests of the symmetry of the pairing state in the high-temperature superconductorsevidence for dx_2-y_2 symmetry,” *Rev. Mod. Phys.*, **67**, 515 (1995).
- [38] C. C. Tsuei and J. R. Kirtley, “Pairing symmetry in cuprate superconductors,” *Rev. Mod. Phys.*, **72**, 969–

- 1016 (2000).
- [39] E. Berg, S. A. Kivelson, and D. J. Scalapino, “A twisted ladder: relating the Fe superconductors to the high- T_c cuprates,” *New Journal of Physics*, **11**, 085007 (2009).
- [40] D. J. Scalapino, “Condensed matter physics - the cuprate pairing mechanism,” *Science*, **284**, 1282–1283 (1999).
- [41] J.P. Hu N. Hao, H. Ding, in preparation (2012).
- [42] L. X. Yang, B. P. Xie, Y. Zhang, C. He, Q. Q. Ge, X. F. Wang, X. H. Chen, M. Arita, J. Jiang, K. Shimada, M. Taniguchi, I. Vobornik, G. Rossi, J. P. Hu, D. H. Lu, Z. X. Shen, Z. Y. Lu, and D. L. Feng, “Surface and bulk electronic structures of LaFeAsO studied by angle-resolved photoemission spectroscopy,” *Phys. Rev. B*, **82**, 104519 (2010).
- [43] D. H. Lu, M. Yi, S.-K. Mo, J. G. Analytis, J.-H. Chu, A. S. Erickson, D. J. Singh, Z. Hussain, T. H. Geballe, I. R. Fisher, and Z.-X. Shen, “Arpes studies of the electronic structure of LaOFeAs,” *Physica C Superconductivity*, **469**, 452–458 (2009).
- [44] Fei Chen, Bo Zhou, Yan Zhang, Jia Wei, Hong-Wei Ou, Jia-Feng Zhao, Cheng He, Qing-Qin Ge, Masashi Arita, Kenya Shimada, Hirofumi Namatame, Masaki Taniguchi, Zhong-Yi Lu, Jiangping Hu, Xiao-Yu Cui, and D. L. Feng, “Electronic structure of Fe_{1.04}Te_{0.66}Se_{0.34},” *Phys. Rev. B*, **81**, 14526 (2010).
- [45] O. J. Lipscombe, G. F. Chen, Chen Fang, T. G. Perring, D. L. Abernathy, A. D. Christianson, Takeshi Egami, Nanlin Wang, Jiangping Hu, and Pengcheng Dai, “Spin waves in the magnetically ordered iron chalcogenide Fe_{1.05}Te,” *Phys. Rev. Lett.*, **106**, 57004 (2011).
- [46] Miaoyin Wang, Chen Fang, Dao-Xin Yao, Guo-Tai Tan, Leland W. Harriger, Yu Song, Tucker Nether-ton, Chenglin Zhang, Meng Wang, Matthew B. Stone, Wei Tian, Jiangping Hu, and Pengcheng Dai, “Spin waves and magnetic exchange interactions in insulating Rb_{0.89}Fe_{1.58}Se₂,” *Nature Comm.*, **2**, 580 (2011).
- [47] P W Anderson, P A Lee, M Randeria, T M Rice, N Trivedi, and F C Zhang, “The physics behind high-temperature superconducting cuprates: the ‘plain vanilla’ version of RVB,” *J. Phys. Cond. Matt.*, **16**, R755 (2004).
- [48] P. A. Lee, N. Nagaosa, and X. G. Wen, “Doping a Mott insulator: Physics of high-temperature superconductivity,” *Reviews of Modern Physics*, **78**, 17–85 (2006).
- [49] J. Zhao, D. T. Adroja, D. X. Yao, R. Bewley, S. L. Li, X. F. Wang, G. Wu, X. H. Chen, J. P. Hu, and P. C. Dai, “Spin waves and magnetic exchange interactions in CaFe₂As₂,” *Nature Physics*, **5**, 555–560 (2009).
- [50] J. Hu, In preparation.
- [51] Y. Zhang, F. Chen, C. He, B. Zhou, B. P. Xie, C. Fang, W. F. Tsai, X. H. Chen, H. Hayashi, J. Jiang, H. Iwasawa, K. Shimada, H. Namatame, M. Taniguchi, J. P. Hu, and D. L. Feng, “Orbital characters of bands in the iron-based superconductor BaFe_{1.85}Co_{0.15}As₂,” *Phys. Rev. B*, **83**, 54510 (2011).
- [52] Fei Chen, Bo Zhou, Yan Zhang, Jia Wei, Hong-Wei Ou, Jia-Feng Zhao, Cheng He, Qing-Qin Ge, Masashi Arita, Kenya Shimada, Hirofumi Namatame, Masaki Taniguchi, Zhong-Yi Lu, Jiangping Hu, Xiao-Yu Cui, and D. L. Feng, “Electronic structure of Fe_{1.04}Te_{0.66}Se_{0.34},” *Phys. Rev. B*, **81**, 14526 (2010).
- [53] Z.-H. Liu and et al., “Three-dimensionality and orbital characters of Fermi surface in (Tl,Rb)_yFe_{2-x}Se₂,” *Arxiv:1202.6417v2* (2012).
- [54] M. F. Jensen, V. Brouet, E. Papalazarou, A. Nicolaou, A. Taleb-Ibrahimi, P. Le Fevre, F. Bertran, A. Forget, and D. Colson, “Angle-resolved photoemission study of the role of nesting and orbital orderings in the antiferromagnetic phase of BaFe₂(As)₂,” *Phys. Rev. B*, **84** (2011).
- [55] Note, The 122 structure doubles unit cell along c-axis. If it is in the B-phase, it requires odd number of iron-layers to measure the sign change. We will discuss this issue in the future.
- [56] G. Kotliar and J. L. Liu, “Superexchange mechanism and d-wave superconductivity,” *Phys. Rev. B*, **38**, 5142 (1988).
- [57] I. R. Fisher, L. Degiorgi, and Z. X. Shen, “In-plane electronic anisotropy of underdoped ‘122’ Fe-arsenide superconductors revealed by measurements of detwinned single crystals,” *Reports on Progress in Physics*, **74**, 124506 (2011).
- [58] C. Fang, H. Yao, W. F. Tsai, J. P. Hu, and S. A. Kivelson, “Theory of electron nematic order in LaFeAsO,” *Phys. Rev. B*, **77**, 224509 (2008).
- [59] Cenke Xu, Markus Müller, and Subir Sachdev, “Ising and spin orders in the iron-based superconductors,” *Phys. Rev. B*, **78**, 20501 (2008).
- [60] Cenke Xu Jiangping Hu, “Review of nematicity in iron based superconductors,” *arxiv:1112.2713* (2012).
- [61] I. I. Mazin and M. D. Johannes, “A key role for unusual spin dynamics in ferropnictides,” *Nature Physics*, **5**, 141–145 (2009).
- [62] F. Krüger, S. Kumar, J. Zaanen, and J. van den Brink, “Spin-orbital frustrations and anomalous metallic state in iron-pnictide superconductors,” *Phys. Rev. B*, **79** (2009).
- [63] Weicheng Lv, Jiansheng Wu, and Philip Phillips, “Orbital ordering induces structural phase transition and the resistivity anomaly in iron pnictides,” *Phys. Rev. B*, **80**, 224506 (2009).
- [64] C. C. Lee, W. G. Yin, and W. Ku, “Ferro-orbital order and strong magnetic anisotropy in the parent compounds of iron-pnictide superconductors,” *Phys. Rev. Lett.*, **103** (2009).
- [65] R. M. Fernandes, E. Abrahams, and J. Schmalian, “Anisotropic in-plane resistivity in the nematic phase of the iron pnictides,” *Phys. Rev. Lett.*, **107** (2011).
- [66] T. A. Maier and D. J. Scalapino, “Pair structure and the pairing interaction in a bilayer Hubbard model,” *arxiv:1107.0401* (2011).